Title

Anirban Mukherjee,[1,*] Abhirup Mukherjee,[1,†] N. S. Vidhyadhiraja,[2,‡] A. Taraphder,[3,§] and Siddhartha Lal[1,¶]

[1] *Department of Physical Sciences, Indian Institute of Science Education and Research-Kolkata, W.B. 741246, India*
[2] *Theoretical Sciences Unit, Jawaharlal Nehru Center for Advanced Scientific Research, Jakkur, Bengaluru 560064, India*
[3] *Department of Physics, Indian Institute of Technology Kharagpur, Kharagpur 721302, India*

(Dated: December 20, 2021)

Lorem ipsum dolor sit amet, consectetuer adipiscing elit. Ut purus elit, vestibulum ut, placerat ac, adipiscing vitae, felis. Curabitur dictum gravida mauris. Nam arcu libero, nonummy eget, consectetuer id, vulputate a, magna. Donec vehicula augue eu neque. Pellentesque habitant morbi tristique senectus et netus et malesuada fames ac turpis egestas. Mauris ut leo. Cras viverra metus rhoncus sem. Nulla et lectus vestibulum urna fringilla ultrices. Phasellus eu tellus sit amet tortor gravida placerat. Integer sapien est, iaculis in, pretium quis, viverra ac, nunc. Praesent eget sem vel leo ultrices bibendum. Aenean faucibus. Morbi dolor nulla, malesuada eu, pulvinar at, mollis ac, nulla. Curabitur auctor semper nulla. Donec varius orci eget risus. Duis nibh mi, congue eu, accumsan eleifend, sagittis quis, diam. Duis eget orci sit amet orci dignissim rutrum.

Nam dui ligula, fringilla a, euismod sodales, sollicitudin vel, wisi. Morbi auctor lorem non justo. Nam lacus libero, pretium at, lobortis vitae, ultricies et, tellus. Donec aliquet, tortor sed accumsan bibendum, erat ligula aliquet magna, vitae ornare odio metus a mi. Morbi ac orci et nisl hendrerit mollis. Suspendisse ut massa. Cras nec ante. Pellentesque a nulla. Cum sociis natoque penatibus et magnis dis parturient montes, nascetur ridiculus mus. Aliquam tincidunt urna. Nulla ullamcorper vestibulum turpis. Pellentesque cursus luctus mauris.

I. INTRODUCTION

II. FIXED POINT THEORY OF THE OVERSCREENED MULTI-CHANNEL KONDO MODEL

A. RG flows towards intermediate coupling

We start with the usual K-channel Kondo model Hamiltonian with isotropic couplings [1]:

$$H = \sum_{l=1}^{K} H_l \ ,$$
$$H_l = \sum_{k} \sum_{\alpha=\uparrow,\downarrow} \epsilon_{k,l} \hat{n}_{k\alpha,l} + J \sum_{kk'} \sum_{\alpha,\beta=\uparrow,\downarrow} \vec{S}_d \cdot \frac{1}{2} \vec{\sigma}_{\alpha\alpha'} c^{\dagger}_{k\alpha,l} c_{k'\alpha',l} \ . \tag{1}$$

Here, l sums over the K channels of the conduction bath, k, k' sum over all the momentum states of the bath and α, β sum over the two spin indices of a single electron. $c_{k\alpha,l}$ is the fermionic field operator at momentum k, spin α and channel l. $\epsilon_{k,l}$ represents the dispersion of the l^{th} conduction channel. $\vec{\sigma}$ is the vector of Pauli matrices and $\vec{S}_d = \frac{1}{2}\vec{\sigma}_d$ is the impurity spin operator.

We have performed a renormalization group analysis of the Hamiltonian using the recently developed URG method [2–7]. The RG proceeds by applying unitary transformations in order to block-diagonalize the Hamiltonian by removing number fluctuations of the high energy degrees of freedom. If the most energetic electronic state at the j^{th} RG step is $|j\rangle$ defined by the energy $D_{(j)}$, the Hamiltonian will in general not conserve the number of particles in this state: $\left[H_{(j)}, \hat{n}_j\right] \neq 0$. The unitary transformation $U_{(j)}$ will remove this number fluctuation at the next RG step:

$$H_{(j-1)} = U_{(j)} H_{(j)} U^{\dagger}_{(j)}, \left[H_{(j-1)}, \hat{n}_j\right] = 0 \tag{2}$$

The unitary transformations are given in terms of a generator $\eta_{(j)}$:

$$U_{(j)} = \frac{1}{\sqrt{2}} \left(1 + \eta_{(j)} - \eta^{\dagger}_{(j)}\right) \tag{3}$$

The generator is fermionic in nature:

$$\left\{\eta_{(j)}, \eta^{\dagger}_{(j)}\right\} = 1, \left[\eta_{(j)}, \eta^{\dagger}_{(j)}\right] = 1 \tag{4}$$

and is given by the expression

$$\eta^{\dagger}_{(j)} = \frac{1}{\hat{\omega}_{(j)} - \text{Tr}\left(H_{(j)} \hat{n}_j\right)} c^{\dagger}_j \text{Tr}\left(H_{(j)} c_j\right) \tag{5}$$

The operator $\hat{\omega}_{(j)}$ encodes the quantum fluctuation scales arising from the interplay of the kinetic energy terms and the interaction terms of the Hamiltonian:

$$\hat{\omega}_{(j)} = H_{(j-1)} - H^{i}_{(j)} \tag{6}$$

$H^{i}_{(j)}$ is that part of $H_{(j)}$ that commutes with $\hat{n}_j$ but does not commute with at least one $\hat{n}_l$ for $l < j$. The RG continues up to energy D^* where a fixed point is reached from the vanishing of either the numerator or the denominator.

* mukherjee.anirban.anirban@gmail.com
† am18ip014@iiserkol.ac.in
‡ raja@jncasr.ac.in
§ arghya@phy.iitkgp.ernet.in
¶ slal@iiserkol.ac.in

The derivation of the RG equation for the overscreened regime ($2S < K$) of the spin-S-impurity K-channel Kondo problem is shown in appendix A. On decoupling circular isoenergetic shells at energies $D_{(j)}$, the change in the Kondo coupling at the j^{th} RG step, $\Delta J_{(j)}$, is given by

$$\Delta J_{(j)} = -\frac{J_{(j)}^2 \mathcal{N}_{(j)}}{\omega_{(j)} - \frac{D_{(j)}}{2} + \frac{J_{(j)}}{4}} \left(1 - \frac{1}{2}\rho J_{(j)} K\right) \quad (7)$$

$\mathcal{N}_{(j)}$ is the number of electronic states at the energy shell $D_{(j)}$. We work in the low quantum fluctuation regime $\omega_{(j)} < \frac{D_{(j)}}{2}$. There are three fixed points of the RG equation. One arises from the vanishing of the denominator, and was present in the single-channel Kondo RG equation as well [8]. As shown there, this fixed-point goes to $J^* = \infty$ as the bare bandwidth of the conduction electrons is made large. The other trivial fixed point is the trivial one at $J^* = 0$. The third fixed point is reached when the numerator vanishes: $J^* = \frac{2}{K\rho}$ [1, 9, 10]. Only the intermediate fixed point is stable [11–16].

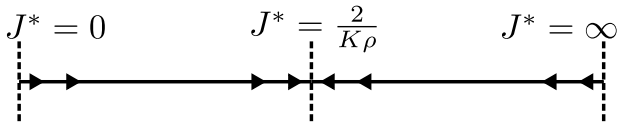

FIG. 1. The three fixed points of the overscreened RG equation. Only the intermediate one is stable.

The RG equation reduces to the perturbative form $\Delta J_{(j)} \simeq \frac{J_{(j)}^2 \mathcal{N}_{(j)}}{D_{(j)}} \left(1 - \frac{1}{2}\rho J_{(j)} K\right)$ [1, 9, 10, 17] when one replaces $\omega_{(j)}$ with the ground state energy $-\frac{D_{(j)}}{2}$ and assumes $J \ll D_{(j)}$.

B. Star graph as the effective fixed point Hamiltonian

The fixed point Hamiltonian takes the form

$$H^* = \sum_l \left[\sum_k^* \epsilon_{k,l} \hat{n}_{k\alpha,l} + J \sum_{kk'}^* \vec{S}_d \cdot \frac{1}{2} \vec{\sigma}_{\alpha\alpha'} c^\dagger_{k\alpha,l} c_{k'\alpha',l} \right] . \quad (8)$$

We have not explicitly written the decoupled degrees of freedom $D_{(j)} > D^*$ in the Hamiltonian. The $*$ over the summations indicate that only the momenta inside the window D^* enter the summation. There is an implied summation over the spin indices α, β.

To study the low energy physics and universality of the problem, we will mostly focus on the zero bandwidth limit of the fixed point Hamiltonian. Upon setting the chemical potential equal to the Fermi energy, this zero bandwidth model becomes a Heisenberg spin-exchange Hamiltonian.

$$H^* = J \sum_l \sum_{kk'}^* \vec{S}_d \cdot \frac{1}{2} \vec{\sigma}_{\alpha\alpha'} c^\dagger_{k\alpha,l} c_{k'\alpha',l} = J \vec{S}_d \cdot \sum_l \vec{s}_l \ . \quad (9)$$

At the last step, we defined the local spin operator $\vec{s}_l = \frac{1}{2}\sigma_l = \frac{1}{2}\sum_{kk'}^* \sum_{\alpha\beta} \vec{\sigma}_{\alpha\alpha'} c^\dagger_{k\alpha,l} c_{k'\alpha',l}$ of each conduction channel. The star graph commutes with several operators, including the total spin operator $J^z = S_d^z + \sum_l s_l^z$ along z, the total bath local spin operator $s^2_{\text{tot}} = \left(\sum_l \vec{s}_l\right)^2$ and the string operators

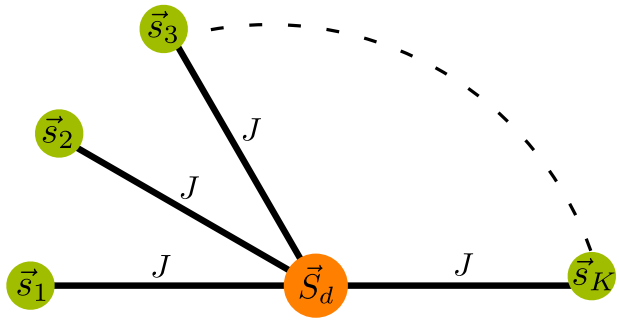

FIG. 2. Zero bandwidth limit of the fixed point Hamiltonian. The central yellow node is the impurity spin, which is talking withe the local spins of the channels represented as green nodes.

$$\pi^{x,y,z} = \sigma_d^{x,y,z} \otimes_{l=1}^K \sigma_l^{x,y,z} \ . \quad (10)$$

The π^z acts on the eigenstates $|J^z\rangle$ and reveals the odd/even parity of the eigenvalue J^z, and is hence a parity operator. Interestingly, the modified string operator $\sigma_d^z \pi^z$ is a Wilson loop that wraps around the outer nodes of the star graph:

$$\pi_c^z \equiv \sigma_d^z \pi^z = \exp\left[i \frac{\pi}{2} \left(\sum_{l=1}^K \sigma_l^z - K \right) \right] \quad (11)$$

π^x and π^y mix states of opposite parity. For example, it can be shown that $\pi^x |J^z\rangle = -|J^z\rangle$. The corresponding modified string operator $\pi_c^x \equiv \sigma_d^x \pi^x$ is an 't Hooft operator [18].

There are multiple reasons for working with specifically the star graph and zero mode Hamiltonians in general. In the URG analysis of the one dimensional Hubbard model [7], a study of the zero mode Hamiltonian (in that case, the Fermi surface itself) was sufficient to topologically characterize various phases of the Berezinskii-Kosterlitz-Thouless (BKT) RG phase diagram. In the single-channel Kondo model, the star graph is just the two spin Heisenberg, and they share the same ground state [19–21] along with thermodynamic properties [8, 19]. Within the MCK model itself, the star graph is able to mimic the nature of the RG flows: At weak coupling $J \to 0^+$, the central spin is weakly coupled to the outer spins and prone to screening because of the $s^\pm$ terms in the star

graph, and at strong coupling $J \to \infty^-$, the outer spin-half objects tightly bind with the central spin-half object to form a single spin object that interacts with the remaining states through an exchange coupling which is RG relevant, rendering both the terminal fixed points unstable. The true stable fixed point must then lie somewhere in between, and we recover the schematic phase diagram of fig. 1. Our claim is that the non-Fermi liquid arises solely from the degeneracy of the ground state manifold of the underlying zero mode Hamiltonian, and the star graph captures the degeneracy in its entirety. The RG flows of the MCK model have been show to *preserve the degeneracy of the ground state* [14, 22, 23]. The star graph conserves the total spin S^z, and this leads to a $K-$fold degeneracy in the ground state of the $K-$channel spin-half star graph which is preserved under the RG flow. This is qualitatively different from the case of the single-channel Kondo model where the $2-$fold degeneracy of the local moment fixed point crosses over into a stable and unique singlet ground state. The importance of the degeneracy can be shown in the following manner. The ground state degeneracy of the more general star graph with a spin-S impurity and K channels is given by $|K-2S|+1$. The cases of $K=2S$, $K<2S$ and $K>2S$ correspond to exactly screened, underscreened and overscreened regimes respectively. The latter two cases correspond to a multiply-degenerate manifold, and simultaneous have non-Fermi liquid phases [1, 11–13, 15, 24–35], while the first regime has a unique ground state and is described by a local Fermi liquid phase [1, 36–39], thereby substantiating the claim that a degeneracy greater than unity leads to non-Fermi liquid physics.

III. IMPORTANT PROPERTIES OF THE STAR GRAPH

A. Spectral and Quantum-mechanical features

B. Measures of entanglement

C. Twist operators and Gauge theories

D. Impurity magnetization and susceptibility: Signatures of quantum criticality

The channel isotropic MCK model is critical; any perturbation away from the perfectly symmetric model in terms of anisotropy is relevant [NEEDS CITATION]. This critical nature leads to several signatures that can be obtained directly from the star graph. These signatures include a discontinuity in the impurity magnetization at zero temperature in the limit of the external field going to zero, and a diverging susceptibility as temperature goes to zero.

We insert a magnetic field that acts only on the impurity and then diagonalize the Hamiltonian.

$$H(h) = J^* \vec{S}_d \cdot \vec{s}_{\rm tot} + h S_d^z \tag{12}$$

The Hamiltonian commutes with $s_{\rm tot}$, so it is already block-diagonal in terms of the eigenvalues M of $s_{\rm tot}$. M takes values in the range $[M_{\rm min}, M_{\rm max}]$, where $M_{\rm max} = K/2$ for a $K-$channel Kondo model, and $M_{\rm min} = 0$ if K is even, otherwise $\frac{1}{2}$. Within each block, the Hamiltonian splits into independent 2×2 blocks characterized by eigenvalues of the total spin operator $J^z = S_d^z + s_{\rm tot}^z$. Defining $\alpha = \frac{1}{2}(Jm+h) + \frac{J}{4}$ and $x_m^M = M(M+1) - m(m+1)$, the partition function can be written as

$$Z(h) = \sum_{M=M_{\rm min}}^{M_{\rm max}} r_M^K \left[\sum_{\substack{m=-M,\\ m\in\mathbb{Z}}}^{M-1} 2e^{\beta\frac{J}{4}} \cosh\beta\sqrt{J^2 x_m^M/4 + \alpha^2} + 2e^{-\beta JM/2}\cosh\beta h/2 \right] \tag{13}$$

Here, $\beta = \frac{1}{k_B T}$, M sums over the eigenvalues of $s_{\rm tot}$ while m sums over $J^z - \frac{1}{2}$ and the additional degeneracy factor r_M^K arises from the possibility that there are multiple subspaces defined by $s_{\rm tot} = M$. This multiplicity is given by

$$r_M^K = {}^{K-1}C_{K/2-M} \tag{14}$$

To calculate the impurity magnetic susceptibility, we will use the expression

$$\chi = \frac{1}{\beta}\lim_{h\to 0}\left[\frac{Z(h)''}{Z(h)} - \left(\frac{Z(h)'}{Z(h)}\right)^2\right] \tag{15}$$

where the $'$ indicates derivative with respect to h. For brevity, we define $\theta_M = \beta J(M+\frac{1}{2})/2$ and $\Sigma_M = \sum_{\substack{m=-M,\\ m\in\mathbb{Z}}}^{M-1}(m+\frac{1}{2})^2$. The derivatives are

$$\lim_{h\to 0} Z(h) = \sum_{M=M_{\rm min}}^{M_{\rm max}} r_M^K \left[4Me^{\beta\frac{J}{4}}\cosh\theta_M + 2e^{-\beta JM/2}\right] \tag{16}$$

$$\lim_{h\to 0}\frac{{\rm d}Z(h)}{{\rm d}h} = 0 \tag{17}$$

$$\lim_{h\to 0}\frac{{\rm d}^2 Z(h)}{{\rm d}h^2} = \frac{\beta^2}{2}\sum_{M=M_{\rm min}}^{M_{\rm max}} r_M^K \left[\frac{e^{\beta\frac{J}{4}}}{\theta_M}\left(2M\sinh\theta_M + \frac{\beta^2 J^2}{4}\left[\frac{\cosh\theta_M}{\theta_M} - \frac{\sinh\theta_M}{\theta_M^2}\right]\Sigma_M\right) + e^{-\beta JM/2}\right] \tag{18}$$

At low temperature $\beta\to\infty$, only the highest value $M_{\rm max}$ will survive:

$$Z \to 2r_{M_{\rm max}}^K M_{\rm max} e^{\beta\frac{J}{2}(M_{\rm max}+1)} \tag{19}$$

$$Z'' \to r_{M_{\max}}^{K} \left(\frac{\beta}{2(M_{\max}+\frac{1}{2})}\right)^{2} e^{\beta\frac{J}{2}(M_{\max}+1)}\Sigma_{M_{\max}} \quad (20)$$

$$\chi \to \frac{\beta\Sigma_{\max}}{2M_{\max}\left(2M_{\max}+1\right)^{2}} = \frac{\beta(K-1)}{12(K+1)} \quad (21)$$

This non-analyticity in a response function is a signature of the critical nature of the Hamiltonian. This is in contrast to the behaviour in the non-critical exactly-screened fixed point where the ground state is unique. There, the susceptibility becomes constant at low temperatures: $\chi(T\to 0) = \frac{W}{4T_K}$, T_K being the single-channel Kondo temperature and W the Wilson number [8, 21, 37, 40].

Another non-analyticity arises when we consider the impurity free energy and the magnetization. The thermal free energy is given by

$$F(h) = -\frac{1}{\beta}\ln Z(h) = -\frac{1}{\beta}\ln\sum_{E_n} e^{-\beta E_n} \quad (22)$$

At $T\to 0$, only the most negative energy $E_{\min}$ survives. Assuming a non-degenerate ground state for $h\neq 0$, the zero temperature free energy becomes

$$F(h\neq 0, T\to 0) = -\frac{1}{\beta}\ln e^{-\beta E_{\min}} = E_{\min} \quad (23)$$

In the star graph Hamiltonian with $K-$channels and in the presence of a field on the impurity (eq. 12), the ground state energy will be one of the negative eigenvalues:

$$\lambda_{m,-}^{M,h} = -J/4 - \frac{1}{2}\sqrt{J^2(M+1/2)^2 + h^2 + 2hJ(m+1/2)} \quad (24)$$

The minimum eigenvalue is obtained by maximizing $h(m+1/2)$. For $h>0$, the ground state is renormalized for the most positive value of m, which is $M-1$. On the other hand, for $h<0$, it occurs for $m=-M$, because that is the most negative value it can take. Among all the values of M, the global ground state is at the largest value of M, $K/2$. Therefore, the minimal energy eigenvalue is

$$E_{\min} = -J/4 - \frac{1}{2}\sqrt{J^2(K+1)^2/4 + h^2 + |h|J(K-1)} \quad (25)$$

The first derivative of the free energy with respect to the field gives

$$F'(h\neq 0, T\to 0) = -\frac{2h + J(K-1)\mathrm{sign}(h)}{4\sqrt{\frac{J^2}{4}(K+1)^2 + h^2 + |h|J(K-1)}} \quad (26)$$

There we used the result that the derivative of $|x|$ is $\mathrm{sign}(x)$. If we now take h to zero from both directions, we get the magnetization of the impurity

$$m = F'(h\to 0^{\pm}, T\to 0) = \mp\frac{1}{2}\frac{(K-1)}{(K+1)} \quad (27)$$

The magnetization is therefore discontinuous as $h\to 0$; it goes to different values depending on the direction in which we take the limit. The only case where it is not analytic is when $K=1$; then the derivative goes to zero from both directions. This non-analyticity has also been verified numerically.

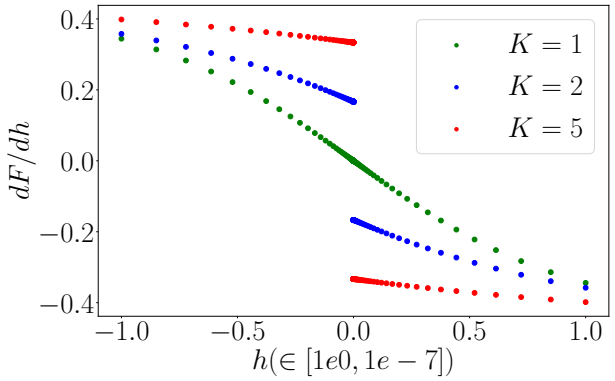

FIG. 3. Non-analytic free energy for $K>1$ and analytic free energy for $K=1$.

The non-analyticity for $K>1$ occurs because the magnetic field is able to flip the ground state. For example, for $K=2$, the states in question are $|M=1, m=-1, 0\rangle$. For $h>0$, the ground state occurs in the subspace $|S_d^z = 1/2, m=-1\rangle, |S_d^z=-1/2, m=0\rangle$. If we now flip the magnetic field, the ground state subspace flips to $|S_d^z=1/2, m=0\rangle, |S_d^z=-1/2, m=1\rangle$. Instead, if we look at the case of $K=1$, the ground state is in the subspace of $|S_d^z=1/2, m=-1/2\rangle, |S_d^z=-1/2, m=1/2\rangle$, and since there is only this one subspace, the ground state is independent of the field. From this discussion, it is clear that the non-analyticity appears because there are multiple values of $m\in[-M, M-1]$ in the ground state manifold, which means that it is the ground state degeneracy that causes the non-analyticity.

E. Impurity magnetization in terms of parity operators

The expectation value of the impurity magnetization along a particular direction and in specific ground states can be related to the 't Hooft operator defined under eq. 11. We will work in the state comprised of two adjacent eigenstates of J^z:

$$|g_{J^z}^{\theta}\rangle \equiv \frac{1}{\sqrt{2}}\left(|J^z\rangle + e^{i\theta}|J^z+1\rangle\right), \quad J^z < \frac{1}{2}(K-1) \quad (28)$$

The expectation value of the impurity magnetization operator σ_d^x can be expressed as

$$\langle\sigma_d^x\rangle \equiv \langle g_{J^z}^{\theta}|\sigma_d^x|g_{J^z}^{\theta}\rangle = -\langle J^z+1|\pi_c^x|-J^z\rangle + \text{h.c.} \quad (29)$$

This expression relates the observable impurity magnetization to the topological 't Hooft operator [41]. Evaluat-

ing the matrix elements gives

$$\langle \sigma_d^x \rangle = -\frac{\sqrt{K^2-(2J^z+1)^2}}{2(1+K)}\cos\theta \tag{30}$$

Performing a similar calculation reveals that the impurity magnetizations along y and z in the same state are given by

$$\langle \sigma_d^y \rangle = -\frac{\sqrt{K^2-(2J^z+1)^2}}{2(1+K)}\sin\theta, \quad \langle \sigma_d^z \rangle = -\frac{2J^z+1}{(1+K)} \tag{31}$$

Combining eqs. 30 and 31, we find

$$\cos^2\theta\left(\langle\sigma_d^x\rangle\right)^2 + \sin^2\theta\left(\langle\sigma_d^y\rangle\right)^2 + \frac{1}{4}\left(\langle\sigma_d^z\rangle\right)^2 = \frac{1}{4}\left(\frac{K}{1+K}\right)^2 \tag{32}$$

This relation constrains the values of the magnetization along all the directions: the x and y magnetization values have already been shown to be related to the 't Hooft operators π^x and π^y and the magnetization along z is therefore constrained in terms of the 't Hooft operators and the quantized function on the right-hand side (the function is quantized because K can only take integer values).

IV. EFFECT OF CONDUCTION BATH EXCITATIONS ON THE FIXED POINT THEORY

A. Non-Fermi liquid effective Hamiltonian

B. Low temperature thermodynamic behaviour

C. Non-Fermi liquid signatures in momentum space

Obtaining the effective Hamiltonian involves obtaining the low energy excitations on top of the ground state of the star graph. The large-energy excitations are ones that involve spin flips. This guides the separation of the Hamiltonian into a diagonal and an off-diagonal piece:

$$H = H_d + V = \underbrace{H_0 + JS_d^z s_{\rm tot}^z}_{H_d} + \underbrace{\frac{J}{2}S_d^+ s_{\rm tot}^- + \text{h.c.}}_{V+V^\dagger} \tag{33}$$

We define V as the interaction term that decreases $s_{\rm tot}^z$ by 1: $V\left|s_{\rm tot}^z\right\rangle \to \left|s_{\rm tot}^z - 1\right\rangle$. Similarly, we define $V^\dagger\left|s_{\rm tot}^z\right\rangle \to \left|s_{\rm tot}^z + 1\right\rangle$. The effective Hamiltonian that has the states $|S_d^z, s_{\rm tot}, s_{\rm tot}^z\rangle$ as eigenstates are

$$H_{\rm eff} = H_d + V\frac{1}{E_{\rm gs}-H_d}V = H_d + \frac{J}{2}S_d^+ s_{\rm tot}^- \frac{1}{E_{\rm gs}-JS_d^z s_{\rm tot}^z - H_0}\frac{J}{2}S_d^- s_{\rm tot}^+ + \frac{J}{2}S_d^- s_{\rm tot}^+ \frac{1}{E_{\rm gs}-JS_d^z s_{\rm tot}^z - H_0}\frac{J}{2}S_d^+ s_{\rm tot}^- \tag{34}$$

This is obtained from the Schrodinger equation for the ground state. If we expand the ground state in terms of $|S_d^z, s_{\rm tot}, s_{\rm tot}^z\rangle$, we have $|\Psi_{\rm gs}\rangle = \sum_{S_d^z, s_{\rm tot}, s_{\rm tot}^z} C_{S_d^z, s_{\rm tot}, s_{\rm tot}^z}|S_d^z, s_{\rm tot}, s_{\rm tot}^z\rangle$. The Schrodinger equation for the ground state can be written as

$$E_{\rm gs}|\Psi_{\rm gs}\rangle = H|\Psi_{\rm gs}\rangle = (H_d+V)|\Psi_{\rm gs}\rangle \implies (E_{\rm gs}-H_d)\sum C_{S_d^z, s_{\rm tot}, s_{\rm tot}^z}|S_d^z, s_{\rm tot}, s_{\rm tot}^z\rangle = V\sum C_{S_d^z, s_{\rm tot}, s_{\rm tot}^z}|S_d^z, s_{\rm tot}, s_{\rm tot}^z\rangle \tag{35}$$

$E_{\rm gs}$ is the ground state energy, and can be replaced by the star graph ground state energy if we remove the kinetic energy cost via normal ordering: $E_{\rm gs} = -\frac{J}{2}\left(\frac{K}{2}+1\right)$. Since the interaction part V only changes $S_d^z \to -S_d^z$ and $s_{\rm tot}^z \to s_{\rm tot}^z \pm 1$, we can simplify the equation into individual smaller equations. For the two-channel model, the possible states are $(s_{\rm tot}, s_{\rm tot}^z) = (0,0),(1,-1),(1,0),(1,1)$. The individual equations for these states are

$$E_{\rm gs}|\frac{1}{2},1,0\rangle = \left(H_d + V\frac{1}{E_{\rm gs}-H_d}V^\dagger\right)|\frac{1}{2},1,0\rangle \tag{36}$$

$$E_{\rm gs}|-\frac{1}{2},1,0\rangle = \left(H_d + V^\dagger\frac{1}{E_{\rm gs}-H_d}V\right)|-\frac{1}{2},1,0\rangle \tag{37}$$

$$\tag{38}$$

These equations represent the Schrodinger equation for the states $|S_d^z,1,0\rangle$, and the right hand sides therefore give the effective Hamiltonians for those states. If we combine the states into a single subspace $|1,0\rangle = \left\{|\frac{1}{2},1,0\rangle, |-\frac{1}{2},1,0\rangle\right\}$, the effective Hamiltonian for this composite subspace becomes the sum of the two parts:

$$H_{\rm eff}^{1,0}|1,0\rangle\langle 1,0| = \left(H_d + VG_0V^\dagger + V^\dagger G_0 V\right)|1,0\rangle \tag{39}$$

where $G_0 = (E_{\rm gs}-H_d)^{-1}$. If we expand the subspace as $|1,0\rangle = |\frac{1}{2},1,0\rangle + |-\frac{1}{2},1,0\rangle$, we recover eqs. 36. Solving similarly for the other states gives

$$H_{\rm eff}^{1,1}|1,1\rangle\langle 1,1| = \left(H_d + V^\dagger G_0 V\right)|1,1\rangle \tag{40}$$

$$H_{\rm eff}^{1,-1}|1,-1\rangle\langle 1,-1| = \left(H_d + VG_0V^\dagger\right)|1,-1\rangle \tag{41}$$

To calculate these effective Hamiltonians, we will calculate the individual terms. We can easily simplify

the S_d^z in the denominator of G_0, because $S_d^{\pm}\frac{1}{A+BS_d^z} = S_d^{\pm}\frac{1}{A\mp\frac{1}{2}B}$:

$$VG_0V^\dagger = \frac{J^2}{4}s_{\rm tot}^-\frac{\frac{1}{2}+S_d^z}{E_{\rm gs}+\frac{J}{2}s_{\rm tot}^z-H_0}s_{\rm tot}^+ \tag{42}$$

$$V^\dagger G_0V = \frac{J^2}{4}s_{\rm tot}^+\frac{\frac{1}{2}-S_d^z}{E_{\rm gs}-\frac{J}{2}s_{\rm tot}^z-H_0}s_{\rm tot}^- \tag{43}$$

Since H_0 does not commute with the spin operators, we will need to expand the denominator to make sense of this Hamiltonian.

$$VG_0V^\dagger = s_{\rm tot}^-\frac{1}{E_{\rm gs}+\frac{J}{2}s_{\rm tot}^z}\left[1+\frac{1}{E_{\rm gs}+\frac{J}{2}s_{\rm tot}^z}H_0+\frac{1}{E_{\rm gs}+\frac{J}{2}s_{\rm tot}^z}H_0\frac{1}{E_{\rm gs}+\frac{J}{2}s_{\rm tot}^z}H_0+\dots\right]s_{\rm tot}^+ \tag{44}$$

$$V^\dagger G_0V = s_{\rm tot}^+\frac{1}{E_{\rm gs}-\frac{J}{2}s_{\rm tot}^z}\left[1+\frac{1}{E_{\rm gs}-\frac{J}{2}s_{\rm tot}^z}H_0+\frac{1}{E_{\rm gs}-\frac{J}{2}s_{\rm tot}^z}H_0\frac{1}{E_{\rm gs}-\frac{J}{2}s_{\rm tot}^z}H_0+\dots\right]s_{\rm tot}^- \tag{45}$$

This is an expansion in $H_0^n/J^{n+1}, n=0,1,2,\dots$. Expanding up to $n=2$ and keeping at most two particle interaction terms, the effective Hamiltonians for these states are:

$$H_{\rm eff}^{1,1} = H_0+JS_d^z+\frac{J^2}{4}\frac{2}{E_{\rm gs}}\left[1+\frac{H_0}{E_{\rm gs}}+\frac{s_{\rm tot}^+X_{1,\rm tot}}{2E_{\rm gs}}+\frac{H_0^2}{E_{\rm gs}^2}-\frac{Z_{1,\rm tot}H_0}{E_{\rm gs}^3}\right]\left(\frac{1}{2}-S_d^z\right) \tag{46}$$

$$H_{\rm eff}^{1,-1} = H_0-JS_d^z+\frac{J^2}{4}\frac{2}{E_{\rm gs}}\left[1+\frac{H_0}{E_{\rm gs}}-\frac{s_{\rm tot}^-X_{1,\rm tot}^\dagger}{2E_{\rm gs}}+\frac{H_0^2}{E_{\rm gs}^2}-\frac{Z_{1,\rm tot}H_0}{E_{\rm gs}^3}\right]\left(\frac{1}{2}+S_d^z\right) \tag{47}$$

$$H_{\rm eff}^{1,0} = H_0+\frac{J^2}{2\left(E_{\rm gs}+\frac{J}{2}\right)}\left[1+\frac{H_0+\left(\frac{1}{2}+S_d^z\right)s_{\rm tot}^+X_{1,\rm tot}-\left(\frac{1}{2}-S_d^z\right)s_{\rm tot}^-X_{1,\rm tot}^\dagger}{2\left(E_{\rm gs}+\frac{J}{2}\right)}+\frac{H_0^2}{\left(E_{\rm gs}+\frac{J}{2}\right)^2}-\frac{Z_{1,\rm tot}H_0}{\left(E_{\rm gs}+\frac{J}{2}\right)^3}\right] \tag{48}$$

We employed the definitions $X_{n,\rm tot} \equiv \sum_l\sum_{k,k'}\left(\epsilon_k-\epsilon_{k'}\right)^n c_{k\downarrow}^\dagger c_{k'\uparrow}, X_{n,l}$ and $Z_{1,\rm tot} \equiv \sum_{k,k',l}\left(\epsilon_k-\epsilon_{k'}\right)\frac{1}{2}\left(c_{k\uparrow,l}^\dagger c_{k'\uparrow,l}-c_{k\downarrow,l}^\dagger c_{k'\downarrow,l}\right)$. Focusing on the effective Hamiltonian for $(1,0)$, we see lots of non-Fermi liquid terms of the form $s_{\rm tot}^+X_{1,\rm tot}, s_{\rm tot}^-X_{1,\rm tot}^\dagger, Z_{1,\rm tot}H_0$. These arise because of the degenerate manifold and the increased availability of states in the Hilbert space for scattering, as compared to the unique singlet ground state of the single-channel Kondo model.

V. STRONG-WEAK DUALITY OF THE GENERAL SPIN-S IMPURITY MULTI-CHANNEL KONDO MODEL

We start from a strong coupling ($J\to\infty$) spin-S impurity MCK Hamiltonian in the over-screened regime ($K>2S$),

$$H(J) = \sum_{k,\sigma,l}\epsilon_{k,l}\hat{n}_{k\sigma,l}+J\vec{S}_d\cdot\vec{s}_{\rm tot}\ . \tag{49}$$

Here, $\vec{s}_{\rm tot}$ is the total spin $\sum_l\sum_{kk'\alpha\beta}\vec{\sigma}_{\alpha\beta}c_{k\alpha,l}^\dagger c_{k'\beta,l}$ of all the zero modes. At strong-coupling, the ground states of the star graph eq. 9 act as a good starting point for a perturbative expansion. As argued previously, there are $K-2S+1$ ground states, labeled by the K values of the total spin angular momentum $S^z = S_d^z+s_{\rm tot}^z = -\frac{K}{2}+S, -\frac{K}{2}+S+1,\dots,\frac{K}{2}-S$. To leverage the large coupling, one can define a new spin impurity $\mathbb{S}$ out of this ground state manifold. Since the degeneracy of a spin is given by its multiplicity $2S'+1$, we have $2S'+1 = K-2S+1 \implies S' = \frac{K}{2}-S$. That is, the spin-$S$ impurity has a dual described by a spin-$(K-2S+1)$ impurity. The states of this new spin are defined by

$$\begin{aligned}\mathbb{S}_d^z\left|S^z\right\rangle &= S^z\left|S^z\right\rangle,\\ \mathbb{S}_d^\pm\left|S^z\right\rangle &= \sqrt{S'\left(S'+1\right)-S^z\left(S^z\pm1\right)}\left|S^z\pm1\right\rangle\end{aligned} \tag{50}$$

The excited states of the star graph can be used to define bosons [22], and the hopping into the lattice can then be re-written using these Bosons. One can then remove the single-particle hoping between the zero modes and the first sites using a Schrieffer-Wolff transformation in the small coupling $J' = \gamma\frac{4t^2}{J}$, and generate an exchange-coupling between the new impurity $\vec{\mathbb{S}}_d$ and the new zero modes formed out of the remaining sites in the lattice [22] (by remaining, we mean those real space sites that have not been consumed into forming the new spin). The new Hamiltonian, characterized by the small super-exchange coupling J', has the form

$$H'(J') = \sum_{k,\sigma,l} \epsilon_{k,l}\hat{n}_{k\sigma,l} + J'\vec{\mathbb{S}}_d \cdot \vec{s'}_{\rm tot} \tag{51}$$

The prime on $s_{\rm tot}$ indicates that it is formed by the new zero modes. This Hamiltonian is very similar to the one in eq. 49, and that is the essence of the strong-weak duality: One can go from the over-screened strong coupling spin-S MCK model to another over-screened weak coupling spin-$(K-2S+1)$ MCK model. For the case of $K = 4S$, we have $S' = S$, and both S_d and $\mathbb{S}_d$ describe the same spin objects (at least formally). The two models are then said to be self-dual. For example, for the case of spin-half MCK model, two-channel model is self-dual.

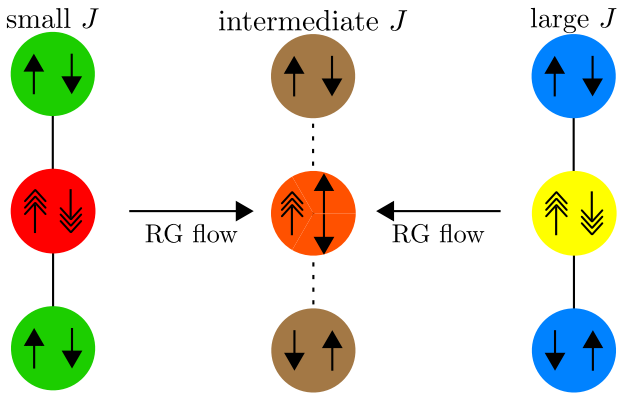

FIG. 4. Duality of the RG flows as seen in the star graph Hamiltonian. The red and green circles represent the impurity and zeroth site spins respectively. At large J, the red circle binds with the green circles to form an effective spin $\frac{K-1}{2}$ object (yellow) that interacts with the remaining spin of the conduction bath (blue circles).

One important consequence of the duality relationship between the two overscreened models is that the RG equations are also dual; while the strong coupling model has an irrelevant coupling J that flows down to the intermediate fixed point J^*, the weak coupling model has a relevant coupling J' that flows up to the same fixed point $J'^* = J^*$. From the RG equation for the general spin-S MCK model, we know that $J'^* = \frac{2}{K\rho'}$, where ρ' is the DOS for the bath of the weak coupling Hamiltonian. This constrains the form of the scaling factor γ:

$$J'^* = \frac{\gamma 4t^2}{J^*} = \frac{2}{K\rho'} \implies \gamma = \frac{1}{4t^2}J^{*2} = \frac{1}{K^2t^2\rho\rho'} \tag{52}$$

VI. IMPURITY QUANTUM PHASE TRANSITION IN THE MULTI-CHANNEL KONDO MODEL UNDER CHANNEL ANISOTROPY

The isotropic MCK mode undergoes a phase transition when the symmetry of the channel interaction strengths is destroyed. It will be shown that if, in a $K-$channel model, one of the couplings becomes slightly larger than the other $K-1$ couplings, the system goes into the singlet ground state characterized by local Fermi liquid excitations. On the other hand, if one of the couplings becomes slightly smaller than the rest, the system goes over to the $K-1$ channel Kondo model.

To see the transition, we need to start with the more general anisotropic MCK model:

$$H = \sum_{k,\alpha,l} \epsilon_{k,l}\hat{n}_{k\alpha,l} + \sum_{kk',\alpha,\beta,l} J_l\vec{S}_d \cdot \frac{1}{2}\vec{\sigma}_{\alpha\beta}c^\dagger_{k\alpha,l}c_{k'\beta,l} \ . \tag{53}$$

Let us consider the specific case where $K-1$ channels have the same coupling $J_1 = J_2 = ... = J_{K-1} = J_+$ and the remaining channel has a different coupling $J_K = J_-$. The RG equations for such a model are

$$\frac{\Delta J_\pm}{|\Delta D|} = -\frac{J_\pm^2\rho}{\mathcal{D}_\pm} + \frac{\rho^2 J_\pm}{2}\left[\frac{(K-1)J_+^2}{\mathcal{D}_+} + \frac{J_-^2}{\mathcal{D}_-}\right] \tag{54}$$

where $\mathcal{D}_\pm = \omega - \frac{D}{2} - \frac{J_\pm}{4}$ are the denominators of the URG equations. Setting $J_+ = J_-$ leads to the critical fixed point at $J_+^* = J_-^* = J_* = \frac{2}{K\rho}$. We now perturb around this fixed point by defining new variables $j_\pm = J_\pm - J_*$. We also assume that the bandwidth is large enough so that $\mathcal{D}_\pm \simeq \omega - \frac{D}{2} - \frac{J_*}{4} = -|\mathcal{D}_*|$. The RG equations then take the form

$$\frac{\Delta j_+}{|\Delta D|} = \frac{\rho J_+}{|\mathcal{D}_*|}\left[J_+ - \frac{\rho}{2}\left[(K-1)J_+^2 + J_-^2\right]\right] = \frac{\rho J_+}{KJ_*|\mathcal{D}_*|}\left[-(K-2)J_*j_+ - (K-1)j_+^2 - j_-^2 - 2J_*j_-\right] \tag{55}$$

$$\frac{\Delta j_-}{|\Delta D|} = \frac{J_-\rho}{|\mathcal{D}_*|}\left[J_- - \frac{\rho}{2}\left[(K-1)J_+^2 + J_-^2\right]\right] = \frac{J_-\rho}{KJ_*|\mathcal{D}_*|}\left[(K-2)J_*j_- - j_-^2 - (K-1)j_+^2 - 2(K-1)J_*j_+\right] \tag{56}$$

We will first look at the special case of $K = 2$, the two channel Kondo model. The equations simplify to

$$\frac{\Delta j_\pm}{|\Delta D|} = \frac{J_\pm \rho}{K J_* |\mathcal{D}_*|} \left[-\left(j_+^2 + j_-^2\right) - 2 J_* j_\mp \right] \tag{58}$$

$$\tag{59}$$

For $j_- < 0, j_+ > 0$, we have $\Delta j_- < 0$. The coupling J_- therefore becomes irrelevant. For small j_+, we have $j_+^2 < 2J_*|j_-|$ and $\Delta j_+ > 0$. This means that the isotropic fixed point is repulsive under anisotropy [1]. The coupling j_+ being relevant means we have a single-channel Kondo problem. We already know the non-perturbative URG equation for the single-channel Kondo problem [8], and it leads to the strong coupling fixed point

We now look at the general K channel case. Let us first look at the regime $j_- < 0, j_+ > 0$. In this regime, we have $\Delta j_- < 0$, which means j_- will flow to larger negative values until it reaches $j_- = -J_*$ such that $J_- = J_* + j_- = 0$. j_+ is, on the other hand, relevant for small values of $j_\pm$. It will continue to grow until the numerator of Δj_+ vanishes. This condition is given by

$$(K-2)\, J_* j_+ + (K-1) j_+^2 + j_-^2 + 2 J_* j_- = 0 \tag{60}$$

Substituting $j_- = -J_*$ gives the fixed-point equation $(K-1) j_+^2 + (K-2)\, J_* j_+ - J_*^2 = 0$. Solving the equation gives

$$j_{+,*} = \frac{J_*}{2(K-1)} \left[-(K-2) \pm K \right] = \frac{J_*}{K-1} \tag{61}$$

At the final step, we chose the positive solution, because j_+ is relevant in this regime. The new fixed point value of J_+ is therefore

$$J_{+,*} = J_* + \frac{J_*}{K-1} = \frac{\frac{2}{K\rho} K}{K-1} = \frac{2}{(K-1)\rho} \tag{62}$$

In other words, the K channel fixed point flows to the $K-1$ channel fixed point. This is shown numerically in fig. 5.

In the opposite regime $j_- > 0, j_+ < 0$, Δj_+ is negative. It has been checked numerically that J_+ ultimately flows to zero in this regime (fig. 6), and J_- remains relevant. Since there is no numerator fixed point in the relevant coupling J_- and because all other couplings are irrelevant, the equation for J_- is replaced by the single-channel Kondo coupling URG equation, and the low-energy physics is then of strong coupling..

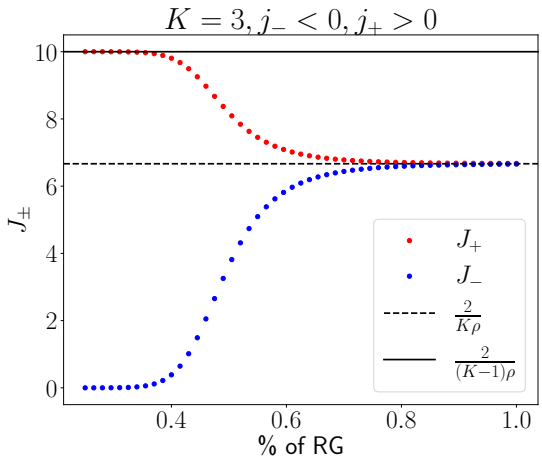

FIG. 5. Flow of J_- to zero when $j_<0$ and J_+ to the fixed point of the $K-1$ channel Kondo model.

VII. CONCLUSIONS

ACKNOWLEDGMENTS

The authors thank P. Majumdar, A. Mitchell, S. Sen, S. Patra, M. Mahankali and R. K. Singh for several discussions and feedback. Anirban Mukherjee thanks the CSIR, Govt. of India and IISER Kolkata for funding through a research fellowship. Abhirup Mukherjee thanks IISER Kolkata for funding through a research fellowship. AM and SL thank JNCASR, Bangalore for hospitality at the inception of this work. NSV acknowledges funding from JNCASR and a SERB grant (EMR/2017/005398).

Appendix A: Hamiltonian RG of spin-S impurity MCK Model

The Hamiltonian for the channel-isotropic MCK model is given in eq. II A. As mentioned in the same section, the Hamiltonian $H_{(j-1)}$ of the $(j-1)^{\text{th}}$ RG step is obtained from the Hamiltonian $H_{(j)}$ of the preceding RG step by applying a unitary transformation $U_{(j)}$: $H_{(j-1)} = U_{(j)} H_{(j)} U_{(j)}^\dagger$. The unitary transformation is obtained in terms of the fermionic operator $\eta_{(j)}$:

$$U_{(j)} = \frac{1}{\sqrt{2}} \left(1 + \eta_{(j)} - \eta_{(j)}^\dagger\right) , \tag{A1}$$

$$\hat{\omega}_{(j)} = H_{(j-1)} - H_{(j)}^i, \; T_{(j)} \equiv \mathrm{Tr}\left(H_{(j)} c_j\right) , \tag{A2}$$

$$\eta_{(j)}^\dagger = \frac{1}{\hat{\omega}_{(j)} - \mathrm{Tr}\left(H_{(j)} \hat{n}_j\right)} c_j^\dagger T_{(j)} . \tag{A3}$$

The operator $\hat{\omega}_{(j)}$ encodes the quantum fluctuation scales arising from the interplay of the kinetic energy terms and the interaction terms of the Hamiltonian.

The URG equation for the single-channel Kondo model [8] shows a stable strong-coupling fixed point. Ferromagnetic interactions are irrelevant. Strictly speaking, that

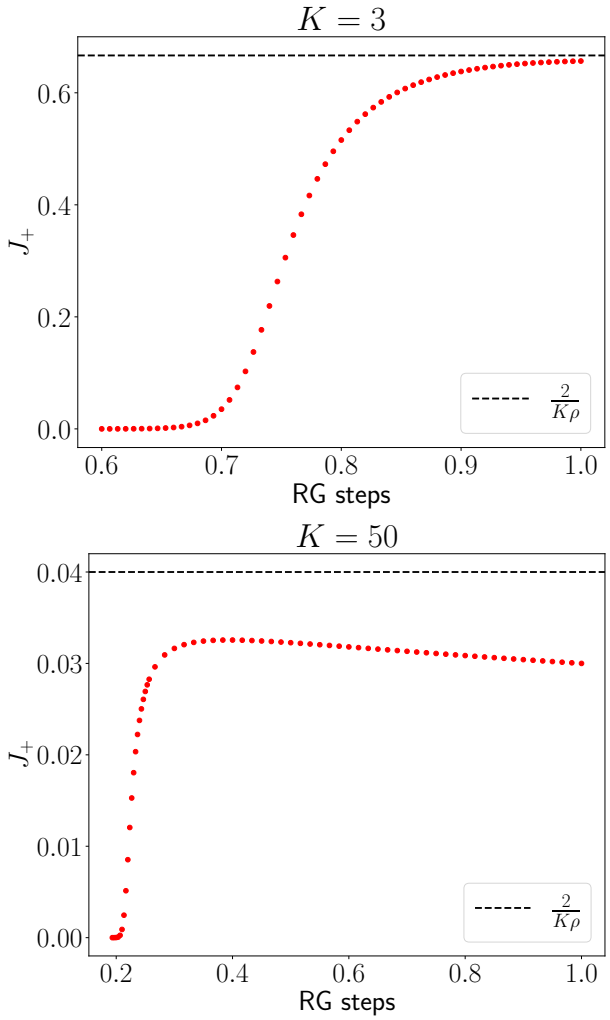

FIG. 6. Flow of the couplings J_+ when $j_+ < 0$ when $j_- > 0, j_+ < 0$, for two values of K.

RG equation already encodes, in principle, the multi-channel behaviour, through a modified $\hat{\omega}$. To extract this information, we consider the strong-coupling fixed-point $J \gg D$ as a fixed point and analyze its stability from the star graph perspective. For the exactly-screened case, the ground state is a singlet and the star graph decouples from the conduction bath, leaving behind a local Fermi liquid interaction on the first site. Similarly, for the underscreened regime, the ground state is composed of states where the impurity spin is only partially screened by the conduction channels. If a particular configuration of the bath-impurity system has the total conduction bath spin down, the impurity will have a residual up spin. The electrons from the nearest sites will hop on to the zeroth site, but they will come with spins up, because the down spin of the conduction channel is already filled. This implies that a ferromagnetic super-exchange coupling is induced, which is irrelevant under RG, so this fixed point is stable as well.

We now come to the overscreened case, where there is a residual spin on the conduction channel site. The neighbouring electrons will now hop in with spins opposite to that of the impurity, so an antiferromagnetic interaction will be induced, and such an interaction is relevant under the RG. This shows that the overscreened regime cannot have a stable strong-coupling fixed point, and we need to search for an intermediate coupling fixed point. We therefore need the generator of the unitary transformation that incorporates third order scattering scatterings explicitly. We should take account of all possible processes that render the set of states $\{|\hat{n}_{q\beta} = 1\rangle, |\hat{n}_{q\beta} = 0\rangle\}$ diagonal. The higher order generator itself has two scattering processes, such that the entire renormalization term $c^\dagger_{q\beta} T\eta$ has in total three coherent processes. The way to make the state $q\beta$ diagonal is to ensure that $c^\dagger_{q\beta} T\eta$ does not change $\hat{n}_{q\beta}$. This is done by letting exactly one of the scattering process in η be $T^\dagger c_{q\beta}$, while the other process in η has to be some internal scattering between the degrees of freedom other than $q\beta$. This, however, does not fix the sequence in which the processes occur within η. Kepeing this in mind, the complete generator upto third order can be written as

$$\eta = \frac{1}{\hat{\omega} - H_D} T^\dagger c \simeq \frac{1}{\omega' - H_D} T^\dagger c + \frac{1}{\omega' - H_D} H_X \frac{1}{\omega' - H_D} T^\dagger c + \frac{1}{\omega' - H_D} T^\dagger c \frac{1}{\omega' - H_D} H_X \tag{A4}$$

where $H_X = J \sum_{k,k'<\Lambda_j,\alpha,\alpha'} \vec{S}_d \cdot \vec{s}_{\alpha\alpha'} c^\dagger_{k\alpha} c_{k'\alpha'}$ is scattering between the entangled electrons. There are two third order terms in the above equation corresponding to the two possible sequences in which the processes can occur while keeping the total renormalization $c^\dagger_{q\beta} T\eta$ diagonal in $q\beta$. With this change, the third order renormalization takes the form

$$\Delta H^{(3)}_j = c^\dagger T \frac{1}{\omega' - H_D} H_X \frac{1}{\omega' - H_D} T^\dagger c + c^\dagger T \frac{1}{\omega' - H_D} T^\dagger c \frac{1}{\omega' - H_D} H_X + \left(c^\dagger \leftrightarrow c, T^\dagger \leftrightarrow T\right) \tag{A5}$$

It is easier to see the RG flow of the couplings if we write the Hamiltonian in terms of the eigenstates of S^z_d. These eigenstates are defined by $S^z_d |m_d\rangle = m_d |m_d\rangle, m_d \in [-S, S]$. In terms of these eigenstates, the Hamiltonian becomes

$$\mathcal{H} = \sum_{k\sigma} \epsilon_k \tau_{k\sigma} + \sum_{m=-S}^{S} \sum_{\substack{kl,\\ \sigma=\uparrow,\downarrow}} J^\sigma_m |m\rangle \langle m| c^\dagger_{k\sigma} c_{l\sigma} + \sum_{kl} \sum_{m=-S}^{S-1} J^t_m \left(|m+1\rangle \langle m| s^-_{kl} + \text{h.c.}\right) \tag{A6}$$

where $J^{\sigma}_{m} = \frac{1}{2}\sigma m J$ in the UV Hamiltonian, and $J^{t}_{m} = J\frac{1}{2}\sqrt{S(S+1) - m(m+1)}$ is the coupling that connects $|m\rangle$ and $|m+1\rangle$.

[1] Nozières, Ph. and Blandin, A., J. Phys. France **41**, 193 (1980).
[2] A. Mukherjee and S. Lal, New Journal of Physics **22**, 063008 (2020).
[3] A. Mukherjee and S. Lal, Nuclear Physics B **960**, 115170 (2020).
[4] A. Mukherjee and S. Lal, Nuclear Physics B **960**, 115163 (2020).
[5] S. Patra and S. Lal, Phys. Rev. B **104**, 144514 (2021).
[6] S. Pal, A. Mukherjee, and S. Lal, **21**, 023019 (2019).
[7] S. P. Anirban Mukherjee and S. Lal, Journal of High Energy Physics **2021** (2021), 10.1007/JHEP04(2021)148.
[8] A. Mukherjee, A. Mukherjee, N. S. Vidhyadhiraja, A. Taraphder, and S. Lal, (2021), arXiv:2111.10580 [cond-mat.str-el].
[9] E. Kogan, Journal of Physics Communications **2**, 085001 (2018).
[10] Y. Kuramoto, The European Physical Journal B - Condensed Matter and Complex Systems **5**, 457 (1998).
[11] I. Affleck and A. W. Ludwig, Nuclear Physics B **360**, 641 (1991).
[12] A. M. Tsvelick and P. B. Wiegmann, Zeitschrift für Physik B Condensed Matter **54**, 201 (1984).
[13] J. Gan, **6**, 4547 (1994).
[14] H. B. Pang and D. L. Cox, Phys. Rev. B **44**, 9454 (1991).
[15] V. J. Emery and S. Kivelson, Phys. Rev. B **46**, 10812 (1992).
[16] J. von Delft, G. Zaránd, and M. Fabrizio, Phys. Rev. Lett. **81**, 196 (1998).
[17] V. Tripathi, Landau Fermi Liquids and Beyond (CRC Press, 2018).
[18] E. Fradkin, Field theories of condensed matter physics (Cambridge University Press, 2013).
[19] C. M. Varma and Y. Yafet, Phys. Rev. B **13**, 2950 (1976).
[20] K. Yosida, Phys. Rev. **147**, 223 (1966).
[21] K. G. Wilson, Reviews of Modern Physics **47**, 773 (1975).
[22] C. Kolf and J. Kroha, Phys. Rev. B **75**, 045129 (2007).
[23] R. Žitko and M. Fabrizio, Phys. Rev. B **95**, 085121 (2017).
[24] J. Gan, N. Andrei, and P. Coleman, Phys. Rev. Lett. **70**, 686 (1993).
[25] A. M. Tsvelick and P. B. Wiegmann, Journal of Statistical Physics **38**, 125 (1985).
[26] O. Parcollet and A. Georges, Phys. Rev. Lett. **79**, 4665 (1997).
[27] T. Kimura and S. Ozaki, Journal of the Physical Society of Japan **86**, 084703 (2017), https://doi.org/10.7566/JPSJ.86.084703.
[28] D. Bensimon, A. Jerez, and M. Lavagna, Phys. Rev. B **73**, 224445 (2006).
[29] D. L. Cox and M. Jarrell, **8**, 9825 (1996).
[30] P. Coleman, L. B. Ioffe, and A. M. Tsvelik, Phys. Rev. B **52**, 6611 (1995).
[31] I. Affleck and A. W. Ludwig, Physical Review B **48**, 7297 (1993).
[32] P. Coleman and C. Pépin, Phys. Rev. B **68**, 220405 (2003).
[33] N. Roch, S. Florens, T. A. Costi, W. Wernsdorfer, and F. Balestro, Phys. Rev. Lett. **103**, 197202 (2009).
[34] A. Schiller and L. De Leo, Phys. Rev. B **77**, 075114 (2008).
[35] P. Durganandini, EPL (Europhysics Letters) **95**, 47003 (2011).
[36] K. G. Wilson, Rev. Mod. Phys. **47**, 773 (1975).
[37] P. Nozieres, Journal of Low Temperature Physics **17**, 31 (1974).
[38] N. Andrei, K. Furuya, and J. H. Lowenstein, Rev. Mod. Phys. **55**, 331 (1983).
[39] A. M. Tsvelick and P. B. Wiegmann, Adv. in Phys. **32**, 453 (1983).
[40] R. Bulla, T. Costi, and T. Pruschke, Rev. Mod. Phys. **80**, 395 (2008).
[41] V. Marić, S. M. Giampaolo, and F. Franchini, Communications Physics **3**, 220 (2020).